

3-D TIME-ACCURATE CFD SIMULATIONS OF A MULTI-MEGAWATT SLENDER BLADED HAWT UNDER YAWED FLOW CONDITIONS

M. Sayed¹

Institute of Aerodynamics and Gasdynamics-IAG
Stuttgart, Baden-Württemberg, Germany

Th. Lutz²

Institute of Aerodynamics and Gasdynamics-IAG
Stuttgart, Baden-Württemberg, Germany

E. Krämer³

Institute of Aerodynamics and Gasdynamics-IAG
Stuttgart, Baden-Württemberg, Germany

ABSTRACT

In the present study, numerical investigations of a Multi-Megawatt slender bladed Horizontal-Axis Wind Turbine (HAWT), under yawed inflow conditions, were conducted using a three-dimensional URANS flow solver based on structured overlapped meshes. The simulations were conducted at different wind speeds of 7 m/sec, 11 m/sec and 15 m/sec when the turbine was at different yaw angles ranging from +60° to -60°. The wake progression under these different yawed conditions were observed. It was found that, the wake deflection angle can be used in the wind farms arrangement in order to reduce the wake losses and improve the overall power performance. It was concluded that, under positive small yaw angle (below $\pm 15^\circ$) the magnitudes of the blade forces are slightly increased. While under high yaw angles (above $\pm 15^\circ$) there is a significant decrease. Moreover, the load fluctuations, for the different yaw angles, has the same frequency but with different amplitude and oscillation shape. It was concluded that at the post-stall case, wind speed of 15 m/sec, there is massive separation with leading edge separation bubbles which might be the reason for more leading edge noise.

INTRODUCTION

As the wind direction is always random and continuously changing, HAWTs are basically exposed to yawed flow conditions most of their operating time. Under these conditions, highly unsteady flow conditions over the wind turbine blades are introduced due to a parallel velocity component to the rotor disk. These unsteadiness results from sturdy radial flow along the span-wise as well as dynamic stall on the blade and also leading edge separation bubbles. As a result, the rotor performance is strongly affected due to the blade load fluctuations which will affect the operational life of the wind turbine due to these load fluctuations. Consequently, it is one of the important aspects to understand the flow unsteadiness under yawed turbine operation conditions for better further development in the future.

Different aerodynamic methods are used to solve the flow field around the wind turbine. These methods varies in their degree of complexity and accuracy ranging from Blade Element Momentum theory (BEM) and lifting line theory [1] to the solution of Navier-Stokes equations using Computational Fluid Dynamics (CFD). Some of literature used simplified method such as the lifting line theory [1] to investigate the aerodynamic loads of the wind turbine under yaw operational conditions. Simulations at yaw angles of 10°, 30° and 60° were performed at wind speed of 10 m/sec. The results showed that the method can't capture the dynamic stall and stall delay and therefore, dynamic stall model should be included to improve the accuracy of the results.

CFD models of wind turbines have been widely used, as in [2, 3, 4, 5, 6, 7 and 8], to accurately capture the flow phenomena that cannot be resolved using simplified numerical methods. CFD simulations of a compressible Euler flow using unstructured meshes are performed in [5]. This aerodynamic model was used because of an inviscid flow assumption at this wind speed. Only one flow case is investigated at yaw angle of 30° and low wind speed of 7 m/sec. Simulations of yawed wind turbine based on the solution the Navier-Stokes

¹ PhD-Candidate, IAG, Stuttgart University, sayed@iag.uni-stuttgart.de

² Dr. Ing. Wind-Energy Group Leader, IAG, Stuttgart University, lutz@iag.uni-stuttgart.de

³ Prof. The head of the Institute, IAG, Stuttgart University, kraemer@iag.uni-stuttgart.de

equations are examined in different literatures. Incompressible structured mesh flow solver combined with a BEM model were used to investigate the wind turbine at a yaw angle of 45° for low wind speed of 7 m/sec [6]. It was concluded that the classical inflow model used in the BEM should be improved to accurately capture the downwash flow of the rotor. Moreover, a hybrid Navier-Stokes/Vortex-wake method coupled to a turbulence model of Baldwin–Lomax were used to investigate the blade loadings at different flow cases [7]. But there were no detailed study on the time-accurate blade loadings.

In the present paper, 3-D time-accurate CFD simulations were conducted on a multi-megawatt HAWT rotor under yawed flow conditions. The flow solver used in this study is called FLOWer which is a block-structured flow solver. Therefore, the computational domain used in the present simulations will be divided into different blocks. It is provided by the German Aerospace Center DLR with specific extensions implemented at the IAG. The simulations are performed at free upwind speeds of 7 m/sec, 11 m/sec and 15 m/sec for different yaw angles ranging from $+60^\circ$ to -60° . The blade surface loads are used to present and compare the time-accurate results and detailed flow features over the blades as also observed.

METHODOLOGY

The wind turbine examined in the present study is the generic reference turbine of the ongoing European InnWind project [9]. It is a large HAWT with 178.3 m rotor diameter. FFA-W3 airfoil series used to design the blade. The blade at the root region is equipped with wedge shaped Gurney flaps to increase the aerodynamic performance [9]. The simulations performed here have been achieved with FLOWer [10] which is a block structured flow solver. Several CFD simulations of different offshore and onshore wind turbines have been conducted using FLOWer at the IAG [11, 12, 13 and 14].

The computational domain of the whole turbine consist of three blades, hub, nacelle and tower. All the domains are placed together and overlapped using CHIMERA overlapping mesh technique, as shown in figure 1. The meshes were generated using Gridgen® which is Pointwise's classic software. For each sub-domain, an independent grid was created with different refinement. Finally a background mesh was created to extend the computational domain to the far field to exclude the effect of the far field on the solution. The grid statistics of the different domains used in the simulations are as shown in table 1 and figures 1 and 2. For the blade mesh, 300 cells were used in the chord-wise direction and 100 cells in the span-wise radial direction. 35 cells were used to resolve the boundary layer with a constant $y^+ \approx 1$ for the first boundary layer cells. The far field distances were used are 6R upstream distance, 9R downstream distance and 6R far field distance and the time-step was equivalent to 3° azimuthal-step. These values were chosen based on studies performed at IAG [14].

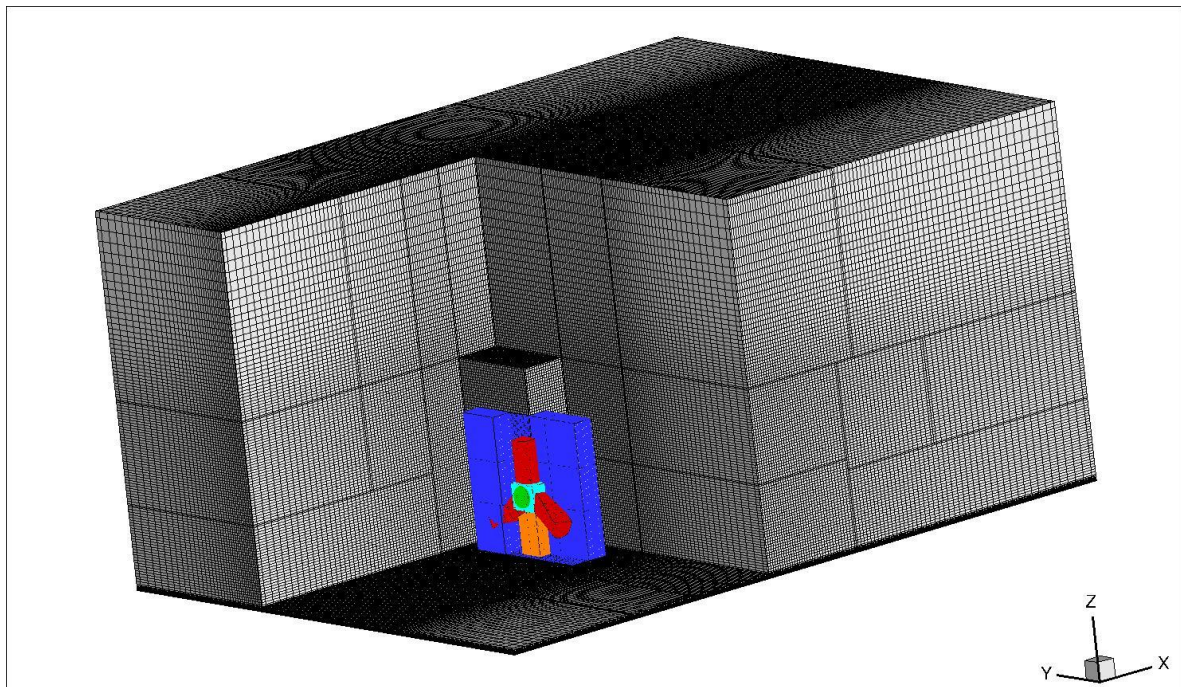


Figure 1. The assembled domains, Red are blades domains, Orange is tower domain, Green is hub domain, Cyan is nacelle domain, Blue is fine background domain and Black is the extended background domain

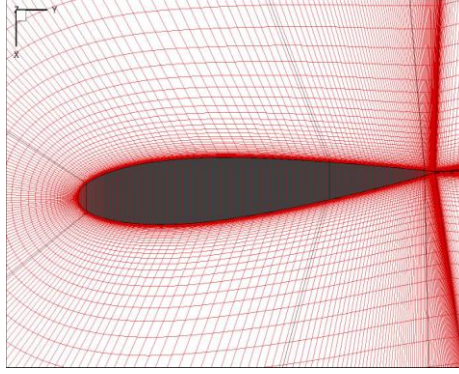


Figure 2. Blade profile meshing

Table 1. Grid statistics

Domain	Blade	Tower	Hub	Nacelle	Fine Background	Extended Background	Blade-hub connector	Total number of cells
Number of cells in millions	6.5	1.15	2.2	1.75	0.9	3.1	0.8	31

The turbulence model used in the simulations is the $k-\omega$ SST (Shear Stress Transport model). The $k-\omega$ SST model has been successfully used to simulate the flow over airfoils and wind turbines. Moreover, it has been used in many wind-turbines CFD studies such as [1, 2 and 14]. All simulations were performed on the Cray XE6 (HLRS) named HORNET using 448 cores.

RESULTS

In the present study, the calculations were made for the wind speeds of 7, 11 and 15 m/sec at the yaw angles ranging from -60° to $+60^\circ$. For each case, the calculation was performed until a periodic unsteady blade aerodynamic loading was converged, which typically requires three rotor revolutions. The time-averaged and unsteady time-varying results for the last rotor revolution are presented in the form of the blade surface pressure and the normal and tangential force coefficients. Detailed flow physics are also analyzed to study the dynamic nature of the rotor behaviors at yaw misalignments.

Wind Speed of 11 m/sec

First of all the simulations were performed at the rated wind speed of 11 m/sec for the yaw angles of -60° , -45° , -30° , -15° , 0° , 15° , 30° , 45° and 60° . 25 revolutions are performed in order to insure the convergence of the load values then the results of the last rotor revolution is presented in this section. Figure 3 shows the azimuthal variations of the power coefficient C_p and the thrust coefficient C_a as. The presented values are firstly result of time-averaging over the last rotor revolution and then normalized by the 0° yaw angle (Baseline). As shown, for a small yaw angles between $+15^\circ$ and -15° there is increase in both values of C_p and C_a with respect to the baseline. The reason for that might be that under these small yaw angles there is stall delay which means more attached flow over the blade in the advancing half of the rotor. Then for the higher yaw angles, sudden decrease in both values, at $\pm 60^\circ$ yaw angle it reaches 30% of the C_p and 60% of the C_a of the baseline.

The loads resulted from the different yawed conditions are also discussed. The azimuthal variation of the normalized thrust and torque are shown in figure 4. The presented values normalized by the 0° yaw angle (Baseline). It can be concluded that, for small yaw angles less than $\pm 30^\circ$, there is a slight change in the thrust compared to the baseline. In contrary, for yaw angles of 45° and 60° , the difference become high and different. For $\pm 45^\circ$ about 7.5% and for $\pm 60^\circ$ about 33% higher value predicted in the advancing half of the rotor. For the torque (figure 4 right), at yaw angle of $\pm 15^\circ$ there is about 20% increase in the advancing half of the rotor, this might be because of the long blade radius. At yaw angle of $\pm 60^\circ$ there is about 40% increase in that half of the rotor.

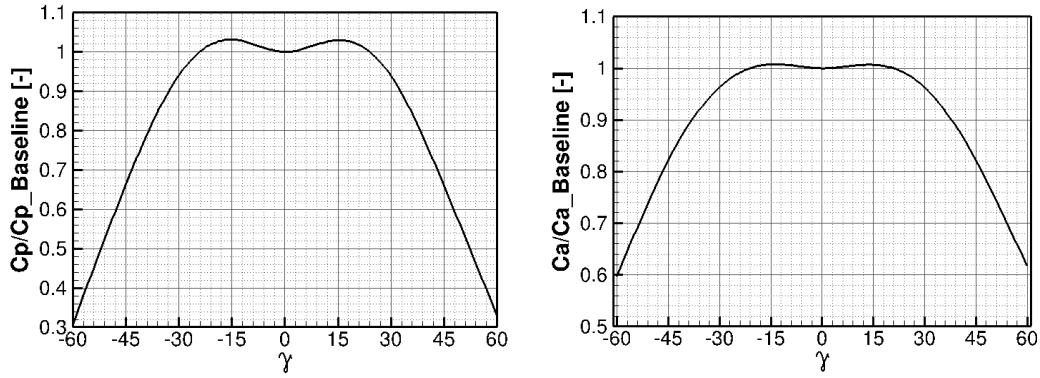


Figure 3. Normalized Power coefficient C_p (left) and Thrust coefficient C_a (right) for different yaw angles.

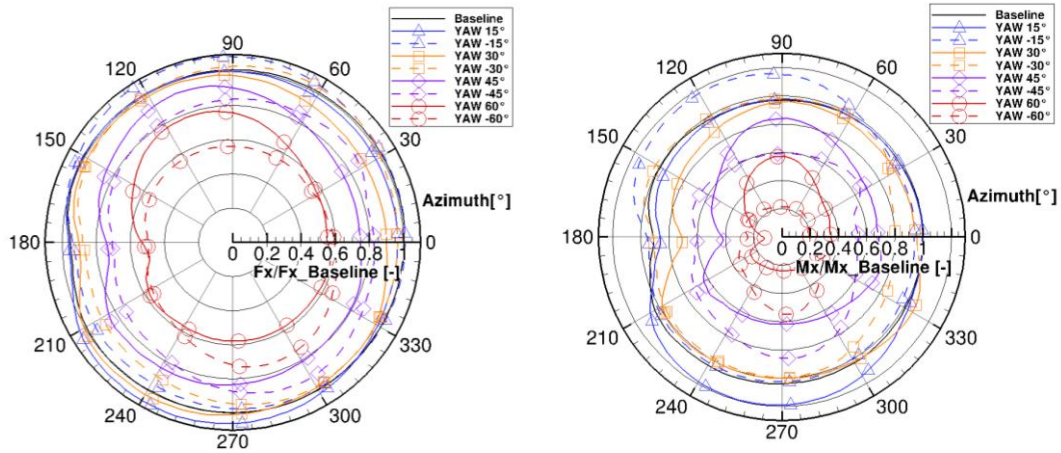


Figure 4. Normalized Thrust (left) and Torque (right) for different yaw angles.

These changes in the loads values might affect the structural vibration of the blades. Therefore, performing Fast Fourier Transform (FFT) will be performed. As shown in figure 5, the first frequency is at 0° Azimuth angle which might be the natural frequency of the wind turbine rotor. For the thrust, the baseline has the smallest amplitude and as the turbine is yawed the amplitude is increased. It can be concluded that the amplitude is higher for the negative yaw compared to the positive one for the same yaw angle except for 60° where both have the same amplitude. In contrast, for the torque, at positive yaw angles the amplitude is slightly higher than at the negative ones. The second, third and fourth frequency are at 180° , 120° and 90° azimuth angles respectively. All the strongest amplitude are in the advancing half on the rotor, which is expecting from the load distribution over one revolution. These high amplitudes will have strong influence on the vibration, fatigue and aero-elastic results and should be taken into account.

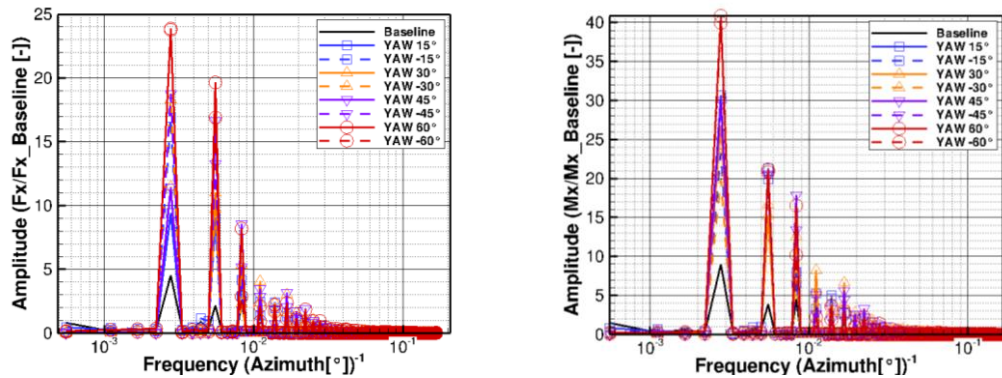


Figure 5. FFT of the normalized Thrust (left) and Torque (right) for different yaw angles.

CONCLUSIONS

In this paper, CFD simulations of a yawed large slender bladed Horizontal-Axis Wind Turbine were conducted using a 3D URANS flow solver based on structured overlapped meshes. Turbulence model of SST has been used for the all simulations. Different yawed conditions have been tested ranging from $+60^\circ$ to -60° . At the rated wind speed of 11 m/sec, time-accurate simulations have been conducted. As the yaw angles increases to $\pm 15^\circ$, the aerodynamic loads over the blades are slightly increased. This might be because of the stall delay results from the reattachment of the flow over the blade surface. As the yaw angle is increased above $\pm 15^\circ$, the aerodynamic loads are significantly reduced. The reason for that is that the wind component become more aligned tangent to the rotor disk plane. The loads fluctuations increase as the yaw angles increase. FFT has been performed and concluded that, the first, second, third and fourth frequency are at 0° , 180° , 120° and 90° azimuth angles respectively. There is a massive increase in the amplitude at higher yaw angles and the strongest amplitudes are in the advancing half on the rotor. These high amplitudes will definitely affect the structure design of the blade and must be taken into account.

ACKNOWLEDGEMENTS

The DAAD (Deutscher Akademischer Austauschdienst) is acknowledged for financial support.

REFERENCES

- [1] Duque EPN, Burklund MD, Johnson W. Navier–Stokes and comprehensive analysis performance predictions of the NREL phase VI experiment. *Journal of Solar Energy Engineering* 2003; 124: 457–467. DOI: 10.1115/1.1624088.
- [2] Sørensen, N. N., Michelsen, J. A. & Schreck S. 2002. Navier–Stokes Predictions of the NREL Phase VI Rotor in the NASA Ames 80 ft x 120 ft Wind Tunnel. *Wind Energy*. Vol. 5 (Issue 2-3): pp. 151–169.
- [3] Hansen, M.O.L., Sørensen, J.N., Voutsinas, S., Sørensen, N. & Madsen, H.Aa. 2006. State of the art in wind turbine aerodynamics and aeroelasticity. *Progress in Aerospace Sciences* 42: pp 285–330.
- [4] Zahle, Frederik & Sørensen, Niels N. 2007. On the Influence of Far-Wake Resolution on Wind Turbine Flow Simulations. *Journal of Physics: Conference Series* 75 (2007) 01204.
- [5] Sezer-Uzol N, Long LN. 3-D time-accurate CFD simulations of wind turbine rotor flow fields, 2006. AIAA Paper 2006–0394.
- [6] Madsen HA, Sørensen NN, Schreck S. Yaw aerodynamics analyzed with three codes in comparisons with experiment, 2003. AIAA Paper 2003–0519.
- [7] Tongchitpakdee C, Benjanirat S, Sankar LN. Numerical simulation of the aerodynamics of horizontal axis wind turbines under yawed flow conditions. *Journal of Solar Energy Engineering* 2005; 127: 464–474.
- [8] Kim DH, Yu DO, Kwon OJ, Fletcher TM, Scheurich F, Brown RE. Predicting unsteady blade loads of a wind turbine using RANS and vorticity transport methodologies. *EWEC 2010, Warsaw 2010*; 2010: 33–37.
- [9] Bak, C., Zahle, F., Bitsche, R., Kim, T., Yde, A., Henriksen, L.C., Andersen, P.B., Natarajan, A. & Hansen, M.H.. Design and performance of a 10 MW wind turbine. *Wind Energy*. To be accepted.
- [10] Kroll, N., Rossow, C.C., Becker, K. & Rhiele F. 2000. *Aerospace Science and Technology*. Vol. 4: pp223-237.
- [11] Bekiropoulos, D., Rieß, R. M., Lutz, Th., Krämer, E., Matha, D., Werner, M. & Cheng P. W. 2012. Simulation of unsteady aerodynamics effects on floating offshore wind turbines. The 11th German Wind Energy conference DEWEK2012.
- [12] Meister, K., Lutz, Th., Krämer, E. 2010. Consideration of unsteady inflow conditions in wind turbine CFD Simulations. The 10th German Wind Energy conference DEWEK2010.
- [13] Schulz, C., Klein, L., Weihing, P., Lutz, Th. & Krämer, E. 2014. CFD Studies on wind turbines in complex terrain under atmospheric inflow conditions. *The Science of Making Torque from Wind*. (2014) 012134.
- [14] Sayed, M., Lutz, Th. & Krämer, E. 2014. Aerodynamic Investigation of Flow over a Multi-Megawatt Slender Bladed Horizontal-Axis Wind Turbine. 1st International Conference on Renewable Energies Offshore. (2014) RENEW2014.